Predicting Local Radiation using Bubble Chambers

Soumadeep Ghosh

Kolkata, India

Abstract

Bubble chambers represent a powerful technology for detecting and characterizing ionizing radiation through the formation of vapor bubbles along particle trajectories. This article examines the theoretical foundations and practical methodologies for predicting local radiation fields using bubble chamber detectors. We discuss the physics of bubble nucleation, calibration techniques, spatial resolution considerations, and computational methods for radiation field reconstruction. The synthesis of experimental data with predictive models enables accurate real-time monitoring of radiation environments across multiple applications, from particle physics research to radiation protection.

The paper ends with "The End"

1 Introduction

The detection and prediction of local radiation fields remains a critical challenge across numerous domains, including nuclear facility monitoring, space exploration, medical physics, and fundamental particle research. Bubble chambers, originally developed by Donald Glaser in 1952, provide a unique approach to radiation detection through the visualization of particle tracks in superheated liquids [1]. Unlike conventional solid-state or gas-filled detectors, bubble chambers offer several advantages: three-dimensional track visualization, sensitivity to neutral particles through secondary interactions, and the ability to discriminate between different radiation types based on track morphology.

The fundamental principle underlying bubble chamber operation involves maintaining a liquid in a metastable superheated state. When ionizing radiation traverses the medium, energy deposition along the particle trajectory creates localized heating that triggers heterogeneous nucleation of vapor bubbles. The spatial distribution, density, and characteristics of these bubbles provide detailed information about the radiation field, enabling both detection and prediction of local radiation environments.

This article presents a comprehensive framework for utilizing bubble chambers in radiation field prediction, incorporating both the microscopic physics of bubble nucleation and macroscopic reconstruction algorithms.

2 Physical Principles of Bubble Chamber Detection

2.1 Thermodynamic Foundation

The operation of bubble chambers relies on maintaining a liquid in a superheated state, where the temperature exceeds the normal boiling point at the prevailing pressure. The degree of superheat, defined as $\Delta T = T - T_{\text{sat}}(P)$, determines the detector's sensitivity to different radiation types. The critical radius for bubble nucleation follows from classical nucleation theory:

$$r_c = \frac{2\sigma}{\rho_v L_v \Delta T / T_{\text{sat}}} \tag{1}$$

where σ represents the surface tension, ρ_v is the vapor density, L_v denotes the latent heat of vaporization, and T_{sat} is the saturation temperature at pressure P.

2.2 Energy Deposition and Nucleation Threshold

Ionizing radiation deposits energy along its trajectory according to the Bethe-Bloch formula for charged particles:

$$-\frac{dE}{dx} = Kz^2 \frac{Z}{A} \frac{1}{\beta^2} \left[\frac{1}{2} \ln \frac{2m_e c^2 \beta^2 \gamma^2 T_{\max}}{I^2} - \beta^2 - \frac{\delta(\beta\gamma)}{2} \right] \tag{2}$$

where $K = 4\pi N_A r_e^2 m_e c^2$, z is the particle charge, Z/A represents the target material properties, $\beta = v/c$, γ is the Lorentz factor, I denotes the mean excitation energy, and $\delta(\beta\gamma)$ accounts for density effect corrections.

The energy required to nucleate a critical bubble, E_{th}, depends on the superheat degree and can be estimated through:

$$E_{\text{th}} = \frac{4\pi r_c^3}{3} \rho_l c_p \Delta T_{\text{eff}} \tag{3}$$

where ρ_l is the liquid density, c_p represents the specific heat capacity, and ΔT_{eff} accounts for thermal diffusion effects during the nucleation timescale.

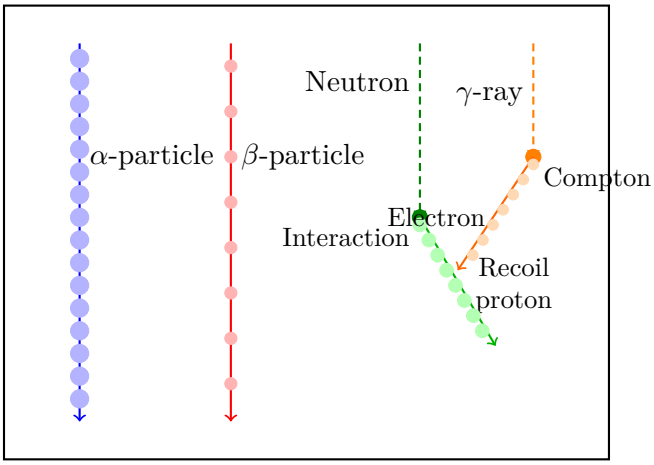

Figure 1: Schematic representation of different radiation types producing characteristic bubble patterns in a bubble chamber.

Alpha particles create dense, straight tracks due to high linear energy transfer. Beta particles produce thinner, sometimes curved tracks with lower bubble density. Neutral particles such as neutrons and gamma rays are invisible until they interact with nuclei or electrons, producing secondary charged particles that create visible bubble tracks. The dashed lines represent the invisible neutral particle paths prior to interaction.

3 Calibration and Response Functions

3.1 Detector Calibration Protocol

Accurate prediction of local radiation fields requires comprehensive calibration of the bubble chamber response. The calibration process establishes the relationship between known radiation sources and measured bubble formation rates. For a monoenergetic source of particle type i with flux Φ_i, the bubble formation rate follows:

$$R_i = \int_{E_{\text{th}}}^{\infty} \Phi_i(E)\sigma_i(E)\epsilon(E)\, dE \tag{4}$$

where $\sigma_i(E)$ represents the energy-dependent cross section for bubble nucleation and $\epsilon(E)$ denotes the detection efficiency.

3.2 Multi-Component Radiation Fields

In realistic environments, radiation fields comprise multiple particle types and energy distributions. The total bubble formation rate becomes:

$$R_{\text{total}} = \sum_i w_i R_i + R_{\text{background}} \tag{5}$$

where w_i represents weighting factors accounting for relative contributions of different radiation components, and $R_{\text{background}}$ captures spontaneous nucleation events.

4 Spatial Resolution and Field Mapping

4.1 Three-Dimensional Track Reconstruction

The intrinsic three-dimensional nature of bubble chambers enables precise spatial localization of radiation events. Stereoscopic imaging from multiple viewing angles allows reconstruction of particle trajectories through triangulation. The spatial resolution δx depends on bubble size, imaging system quality, and reconstruction algorithms:

$$\delta x \approx \sqrt{\delta x_{\text{bubble}}^2 + \delta x_{\text{optical}}^2 + \delta x_{\text{algorithm}}^2} \tag{6}$$

Typical modern bubble chambers achieve spatial resolutions ranging from 100 micrometers to 1 millimeter, depending on the specific implementation and operating conditions.

4.2 Radiation Field Tomography

By accumulating bubble formation data over time and spatial positions, one can reconstruct the three-dimensional radiation field distribution through tomographic techniques. The radiation field $\Phi(\mathbf{r}, E, t)$ can be expressed as:

$$\Phi(\mathbf{r}, E, t) = \sum_j \alpha_j \phi_j(\mathbf{r}, E) + \Phi_{\text{ambient}}(E) \tag{7}$$

where ϕ_j represents basis functions (often Gaussian or finite element bases), α_j are coefficients determined through inverse problem solving, and Φ_{ambient} accounts for uniform background contributions.

`The following space was deliberately left blank.`

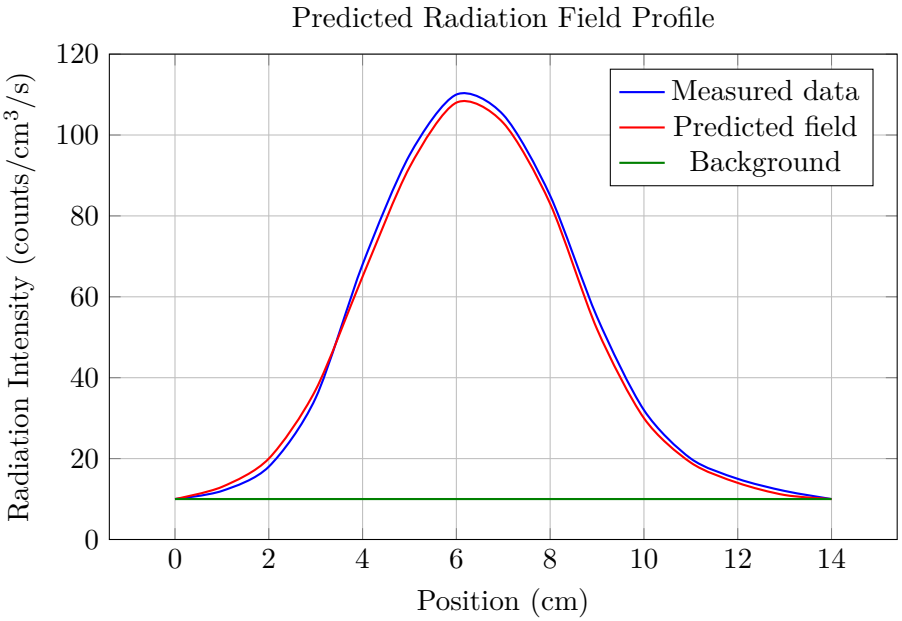

Figure 2: Comparison of measured bubble formation data with predicted radiation field profile.

The peak represents a localized radiation source, while the background level indicates ambient radiation. The predicted field (red dashed line) closely matches measured data (blue solid line) after calibration and field reconstruction.

5 Computational Methods for Radiation Prediction

5.1 Forward Modeling

Forward modeling involves predicting the expected bubble chamber response given a known or hypothesized radiation field. This approach employs Monte Carlo radiation transport codes coupled with nucleation physics. The simulation workflow comprises several steps: generation of radiation source terms, particle transport through the detector geometry, calculation of energy deposition along particle trajectories, and evaluation of nucleation probability at each deposition site.

The nucleation probability P_{nuc} at a given energy deposition site can be modeled through:

$$P_{\text{nuc}}(E_{\text{dep}}) = 1 - \exp\left(-\frac{E_{\text{dep}} - E_{\text{th}}}{\Delta E_{\text{char}}}\right) \quad \text{for } E_{\text{dep}} > E_{\text{th}} \tag{8}$$

where ΔE_{char} represents a characteristic energy scale related to thermal fluctuations and nucleation kinetics.

5.2 Inverse Problem and Field Reconstruction

The inverse problem involves determining the radiation field distribution that best explains observed bubble formation patterns. This constitutes an ill-posed inverse problem typically addressed through regularized optimization. The objective function to minimize takes the form:

$$J[\Phi] = \|\mathbf{A}\Phi - \mathbf{d}\|^2 + \lambda \mathcal{R}[\Phi] \tag{9}$$

where $\mathbf{A}$ represents the forward operator mapping radiation fields to detector responses, $\mathbf{d}$ contains the measured data, λ is the regularization parameter, and $\mathcal{R}[\Phi]$ denotes a regularization functional promoting physically reasonable solutions (such as smoothness or sparsity).

Iterative algorithms such as conjugate gradient methods, algebraic reconstruction techniques, or Bayesian inference approaches provide practical computational frameworks for solving these inverse problems.

5.3 Machine Learning Approaches

Recent advances in machine learning offer complementary approaches to radiation field prediction. Convolutional neural networks trained on extensive datasets of bubble chamber images and corresponding radiation fields can learn complex mappings between observed patterns and underlying radiation distributions. These data-driven methods excel at pattern recognition tasks and can identify subtle correlations that may be challenging to capture through purely physics-based models.

6 Applications and Case Studies

6.1 Dark Matter Detection

Bubble chambers employing superheated noble liquids or hydrocarbons serve as sensitive detectors for weakly interacting massive particles (WIMPs). The predicted local radiation background, particularly from neutron sources, critically influences detection sensitivity and false-positive rates. Accurate radiation field prediction enables optimization of shielding configurations and identification of signal regions with minimal background contamination [6].

6.2 Neutron Dosimetry

Neutron radiation poses particular challenges for dosimetry due to the absence of direct ionization. Bubble detectors provide tissue-equivalent neutron dosimetry through hydrogenous target fluids. Calibration against known neutron fields enables prediction of dose equivalent rates in workplace environments, nuclear facilities, and medical treatment rooms [3].

6.3 Space Radiation Monitoring

The complex radiation environment in space, comprising galactic cosmic rays, solar energetic particles, and trapped radiation belt populations, necessitates robust monitoring capabilities. Bubble chambers deployed on spacecraft or space stations can measure radiation fields and predict astronaut dose accumulation. The three-dimensional tracking capability enables discrimination between different radiation components and estimation of linear energy transfer distributions relevant to biological effects [7].

7 Systematic Uncertainties and Limitations

7.1 Temperature and Pressure Stability

Bubble chamber sensitivity exhibits strong dependence on thermodynamic conditions. Temperature fluctuations of order 0.1 Kelvin can significantly alter the nucleation threshold and detection efficiency. Maintaining precise temperature control throughout the detector volume represents an ongoing technical challenge. Similarly, pressure variations affect the degree of superheat and must be carefully monitored and compensated in radiation field predictions.

7.2 Bubble Coalescence and Multiple Scattering

At high radiation intensities, individual bubbles may coalesce before detection, leading to undercounting and distortion of spatial information. Multiple scattering of charged particles

within dense media introduces additional trajectory uncertainties that degrade spatial resolution. These effects require careful consideration in field reconstruction algorithms, particularly for high-dose-rate environments.

7.3 Neutral Particle Detection Efficiency

While bubble chambers can detect neutral particles through secondary charged particle production, the detection efficiency depends on interaction cross sections and secondary particle ranges. Neutron detection efficiency varies with neutron energy and target composition, typically exhibiting maximum sensitivity in the thermal to epithermal energy range for hydrogenous targets. Gamma-ray detection requires sufficient interaction probability for Compton scattering or pair production, limiting sensitivity at lower energies.

8 Future Developments and Outlook

Continued advancement in bubble chamber technology and radiation field prediction methods proceeds along several promising directions. Development of novel superheated fluids with tailored thermodynamic properties enables optimization for specific radiation types and energy ranges. Integration of real-time image analysis through edge computing and artificial intelligence algorithms facilitates immediate radiation field characterization and hazard identification.

Miniaturization of bubble chamber systems through microfluidic fabrication techniques opens possibilities for distributed sensor networks providing comprehensive spatial coverage. Such networks could revolutionize radiation monitoring in nuclear facilities, medical centers, and research laboratories by providing continuous three-dimensional mapping of radiation fields.

The combination of advanced computational modeling, improved detector technologies, and sophisticated data analysis methods positions bubble chambers as powerful tools for radiation field prediction across diverse applications. As computational capabilities continue to expand and our understanding of nucleation physics deepens, the accuracy and reliability of radiation predictions will correspondingly improve.

9 Conclusion

Bubble chambers provide a versatile platform for detecting and predicting local radiation fields through visualization of particle interactions in superheated liquids. The integration of fundamental nucleation physics, calibration protocols, spatial reconstruction algorithms, and computational inverse problem solving enables quantitative characterization of complex radiation environments. Applications spanning fundamental physics research, radiation protection, and space exploration demonstrate the broad utility of this detection approach.

The predictive capability emerges from careful calibration against known sources, development of accurate response functions across radiation types and energies, and application of sophisticated mathematical techniques for field reconstruction from sparse measurements. While systematic uncertainties related to thermodynamic stability, bubble coalescence, and neutral particle detection efficiency require careful treatment, modern bubble chamber systems achieve impressive performance in terms of sensitivity, spatial resolution, and radiation type discrimination.

Future developments in detector technology, computational methods, and machine learning approaches promise further enhancements in radiation field prediction accuracy and real-time monitoring capabilities. The continued evolution of bubble chamber technology ensures its relevance for emerging applications in radiation science and technology.

References

[1] Glaser, D. A. (1952). Some effects of ionizing radiation on the formation of bubbles in liquids. *Physical Review*, 87(4), 665.

[2] Seitz, F. (1958). On the theory of the bubble chamber. *The Physics of Fluids*, 1(1), 2-13.

[3] Ing, H., Noulty, R. A., & McLean, T. D. (1997). Bubble detectors—a maturing technology. *Radiation Measurements*, 27(1), 1-11.

[4] Apfel, R. E. (1979). The superheated drop detector. *Nuclear Instruments and Methods*, 162(1-3), 603-608.

[5] Barnabé-Heider, M., et al. (2005). Response of superheated droplet detectors of the PICASSO dark matter search experiment. *Nuclear Instruments and Methods in Physics Research Section A*, 555(1-2), 184-204.

[6] Amole, C., et al. (2017). Dark matter search results from the complete exposure of the PICO-60 C_3F_8 bubble chamber. *Physical Review D*, 100(2), 022001.

[7] Zeitlin, C., et al. (2013). Measurements of energetic particle radiation in transit to Mars on the Mars Science Laboratory. *Science*, 340(6136), 1080-1084.

[8] Harper, M. J., & Nelson, W. R. (2003). The use of bubble detectors for neutron dosimetry. *Radiation Protection Dosimetry*, 106(1), 61-66.

[9] Behnke, E., et al. (2013). First measurement of the spin-dependent cross section in the COUPP dark matter search experiment. *Physical Review Letters*, 106(2), 021303.

The End